α-Helical Peptides

Deutsche Ausgabe: DOI: 10.1002/ange.201602079
Internationale Ausgabe: DOI: 10.1002/anie.201602079

Helix Nucleation by the Smallest Known α-Helix in Water

Huy N. Hoang[+], Russell W. Driver[+], Renée L. Beyer, Timothy A. Hill, Aline D. de Araujo, Fabien Plisson, Rosemary S. Harrison, Lena Goedecke, Nicholas E. Shepherd, and David P. Fairlie**

Abstract: *Cyclic pentapeptides (e.g. Ac-(cyclo-1,5)-[KAXAD]-NH_2; X = Ala, **1**; Arg, **2**) in water adopt one α-helical turn defined by three hydrogen bonds. NMR structure analysis reveals a slight distortion from α-helicity at the C-terminal aspartate caused by torsional restraints imposed by the K(i)–D(i + 4) lactam bridge. To investigate this effect on helix nucleation, the more water-soluble **2** was appended to N-, C-, or both termini of a palindromic peptide ARAARAARA (≤ 5 % helicity), resulting in 67, 92, or 100 % relative α-helicity, as calculated from CD spectra. From the C-terminus of peptides, **2** can nucleate at least six α-helical turns. From the N-terminus, imperfect alignment of the Asp5 backbone amide in **2** reduces helix nucleation, but is corrected by a second unit of **2** separated by 0–9 residues from the first. These cyclic peptides are extremely versatile helix nucleators that can be placed anywhere in 5–25 residue peptides, which correspond to most helix lengths in protein–protein interactions.*

Over 30 % of protein structure is composed of helical sequences that stabilize tertiary structure, influence folding, form enzyme active sites, and mediate interactions with other proteins to effect function.[1] Viruses, bacteria, and toxins also use α-helices to fuse with and infect host cells.[2] Protein α-helices interact with other proteins, peptides, RNA, DNA, metal ions, and organic compounds,[1] usually through 1–4 helical turns[3a] and one helical face.[3b] Short synthetic peptides do not form thermodynamically stable α-helices in water, which competes for helix-defining hydrogen-bonding backbone amides, and so do not reproduce bioactive protein helices. Approaches to stabilize peptide helicity include the cross-linking of amino acid side chains by using a disulfide,[4a] thioether,[4b,c] oxime,[4d] lactam,[5,6] or hydrocarbon "staple";[7,8] the replacement of an α-helix-defining (i, i + 4) hydrogen bond with a covalent bond;[9,10] the use of β-amino acids or peptoids as helical foldamers;[11] and the use of conformationally restricted organic scaffolds[12] or metal-ion clips[13] in helix mimics. Each strategy has limitations, such as conformational plasticity, hydrophilicity, synthetic difficulties, inaccurate mimicry of H-bonds, or unidirectional helix induction.

In this study, we examined in detail the helix-inducing propensity of Ac-(cyclo-1,5)-[KAXAD]-NH_2 (X = A, **1**; R, **2**), which is the smallest known[6a–c] α-helical peptide in water (Figure 1 A), has the most effective α-helix-inducing (i, i + 4) linker,[6b,d] and is resistant to strong denaturing conditions.[6b]

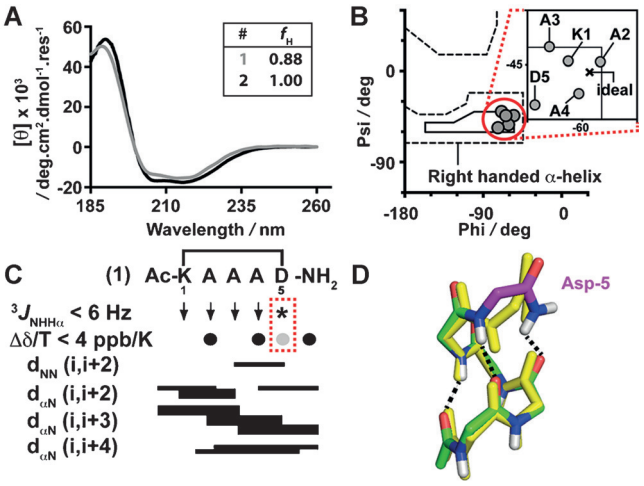

Figure 1. A) CD spectra of **1** and **2** in 10 mM aqueous phosphate buffer (pH 7.4, 298 K). Fractional helicity, f_H, was calculated as described previously.[6b] B) Ramachandran plot for residues in the average NMR structure of **1**. All residues fall within α-helical space. C) NMR features of **1**. The red box highlights unusual data, which suggest a distortion at the C-terminus (*: $^3J_{NH-CH\alpha}$ = 6.9 Hz; gray dot: $\Delta\delta/T$ = 4.8 ppb/K). D) Idealized α-helix (yellow) superimposed on a representative NMR structure of **1** (green) showing that Asp5 (magenta) in **1** deviates slightly from idealized α-helicity.

We found a very small distortion in the helix at the C-terminal Asp residue and investigated its effect on helix induction from the N- versus C-terminus of an appended peptide. The findings highlight how a very subtle torsional change at just one amide bond can become amplified in polypeptides, leading to important structural changes. This information expands our understanding of peptide and protein folding and can help the optimization of small peptide mimics of biologically important protein α-helices.

The NMR-derived structure of **1** in H_2O/D_2O (9:1) at 298 K (see Figure S10 and Tables S7–S9 in the Supporting Information) was canonically α-helical, with all residues in the Ramachandran plot corresponding to right-handed α-

[*] Dr. H. N. Hoang,[+] Dr. R. W. Driver,[+] Dr. R. L. Beyer, Dr. T. A. Hill, Dr. A. D. de Araujo, Dr. F. Plisson, Dr. R. S. Harrison, L. Goedecke, Dr. N. E. Shepherd, Prof. D. P. Fairlie
Division of Chemistry and Structural Biology and
ARC Centre of Excellence in Advanced Molecular Imaging,
Institute for Molecular Bioscience, The University of Queensland
Brisbane, QLD 4072 (Australia)
E-mail: n.shepherd@imb.uq.edu.au
d.fairlie@imb.uq.edu.au

[+] These authors contributed equally to this work.

Supporting information for this article can be found under: http://dx.doi.org/10.1002/anie.201602079.

helicity (Figure 1B). However, some NMR data suggested that the lactam-forming Asp5 residue deviated slightly from ideal helicity (Figure 1C). First, its $^3J_{NH-CH\alpha}$ coupling was high (6.9 Hz), as in a random coil. Second, the $\Delta\delta/T$ value for the Asp5 amide proton was higher (4.8 ppb/K) than normal (4 ppb/K) for a hydrogen bond (to Lys1 CO). These data suggest a slight perturbation in the Asp5 dihedral angles, as corroborated by flexibility observed in NMR structures of **1** (see Figure S10) and deviations in individual backbone and Cβ atoms from ideal α-helicity (Figure 1D). This distortion had little impact on the α-helicity of **1** and **2** as judged by CD spectra (Figure 1A), but we wondered if it could affect torsion angles of Asp5 and misalign amides to restrict α-helix nucleation in attached peptides.

To investigate the importance of this distortion, the more water soluble Ac-(cyclo-1,5)-[KARAD]-NH_2 (**2**) was evaluated as both an N- and C-terminal helix nucleator when attached to a palindromic nonapeptide, ARAARAARA. The CD spectrum of Ac-ARAARAARAKARAD-NH_2 (**3**) was compared with those of N-capped Ac-(cyclo-1,5)-[KARAD]ARAARAARA-NH_2 (**4**) and C-capped Ac-(cyclo-10,14)-ARAARAARA[KARAD]-NH_2 (**5**) in 10 mM phosphate buffer (pH 7.4, 298 K; Figure 2). CD and ^{1}H NMR spectra

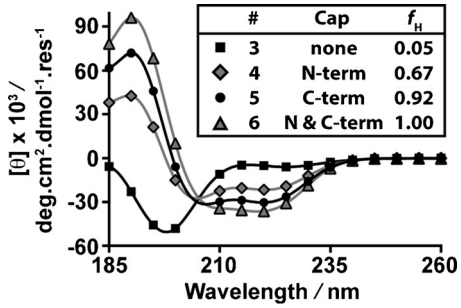

Figure 2. CD spectra of **3** (squares), **4** (diamonds), **5** (circles), and **6** (triangles) in aqueous 10 mM phosphate buffer (pH 7.4, 298 K). Cap refers to the position at which **2** is appended to **3**; $f_H = ([\theta]_{222}-[\theta]_0)/([\theta]_{max}-[\theta]_0)$, in which $[\theta]_{max} = (-44\,000 + 250\,T)(n-x)/n$ and n = number of residues, $x = 2$, $[\theta]_0 = (2220-253\,T)$.

(see Figure S11) excluded the possibility of concentration-dependent aggregation, which can alter helical line shapes. The CD line shape for **3** was consistent with a "random coil" conformation with a single minimum at $\lambda = 198$ nm. The line shapes for **4** and **5** were more α-helical, although the molar residue ellipticity at $\lambda = 222$ nm for **5** was greater than for **4**. Calculated fractional helicities implied that attached residues were also α-helical. Thus, the cyclic pentapeptide **2** was able to propagate helicity from both N- and C-termini. However, on the basis of CD spectral line shapes, **2** was a more effective α-helix nucleator at the C-terminus than at the N-terminus of ARAARAARA (i.e. **5** vs. **4**).

NMR experiments showed that when the cyclic peptide was at the C-terminus (in **5**), more residues had α-helix-like amide coupling constants ($^3J_{NH-CH\alpha} < 6.0$ Hz) and variable-temperature coefficients consistent with intramolecular hydrogen bonds (< 4.0 ppb/K$^<$),[14] than for the N-capped peptide **4** (Figure 3A, see also Tables S16 and S23). Addi-

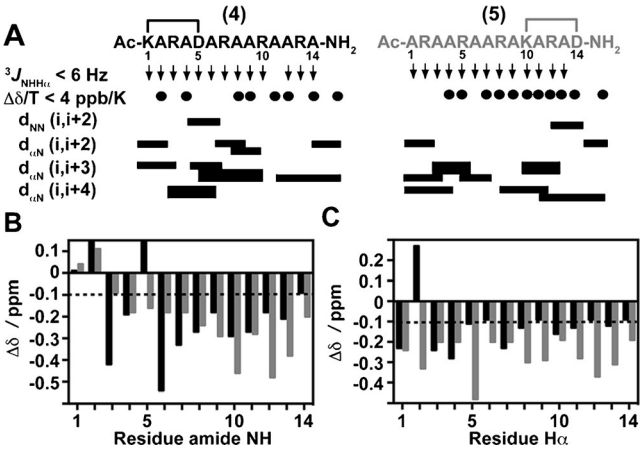

Figure 3. Summary of the helix-defining ^{1}H NMR characteristics of peptides **4** (black) and **5** (gray). A) Amide coupling constants ($^3J_{NH-CH\alpha}$), temperature coefficients ($\Delta\delta/T$), ROE cross-peaks. C, B) Chemical-shift changes ($\Delta\delta$, ppm) from linear-peptide values for amide NH (B) and Hα protons (C) for peptides **4** and **5** in H_2O/D_2O (9:1) at 298 K. The dotted line indicates the threshold for helicity.

tionally, more $d_{\alpha N}(i,i+3)$ and $d_{\alpha N}(i,i+4)$ ROE cross-peaks consistent with α-helicity were observed in the acyclic chain of **5** than in **4** (Figure 3A), which also had $d_{\alpha N}(i,i+2)$ and $d_{NN}(i,i+2)$ cross-peaks around Asp5. Amide NH and Hα chemical shifts of residues in **4** and **5** were > 0.1 ppm lower than typical values for a linear peptide, although chemical-shift differences for **5** were more negative (Figure 3B,C).

Thus, α-helix induction in a peptide by cyclic peptide **2** was more efficient from the C- than from the N-terminus, according to multiple NMR parameters. These data corroborated CD spectra (Figure 2), which suggested that α-helicity extended throughout **5** and through part of **4**, although the distal residues lacked $(i,i+4)$ hydrogen-bonding partners and were not held tightly in an α-helix, thus translating to weaker CD ellipticity. To investigate the hydrogen-bonding network in **4** and **5** in more detail, we studied variable-temperature NMR chemical shifts. The amide NH group in 11 residues of **5** but only 8 residues of **4** had low temperature coefficients (< 4.0 ppb/K), consistent with more intramolecular hydrogen bonds in **5** than **4**. Peptide **4** had some high temperature coefficients ($\Delta\delta/T$: Ala6, 6.6 ppb/K; Arg7, 5.0 ppb/K; Asp5, 13.7 ppb/K), thus suggesting that these amide NH groups were not hydrogen-bonded, or that subtle structural changes contributed to lower overall α-helicity.

To better understand α-helix induction, we also calculated the solution structures of **4** and **5** in water (Figure 4). The structure for **4** in H_2O/D_2O (9:1) at 298 K (see Figure S32A and Table S18) had a larger average pairwise backbone root-mean-square deviation (RMSD 1.62 Å) than **5** (RMSD: 1.35 Å) from an idealized helix (Figure 4A). While the N- and C-termini were α-helical, residues closest to the cycle were distorted with two $(i,i+4)$ residue pairs, Arg3/Arg7 and Ala2/Ala6, missing hydrogen bonds. The Ramachandran plot for **4** (Figure 4B) showed these residues bordering or outside α-helical space and not optimally positioned for hydrogen bonding. An NMR structure for **5** in H_2O/D_2O (9:1) at 298 K was canonically α-helical, with an average backbone RMSD

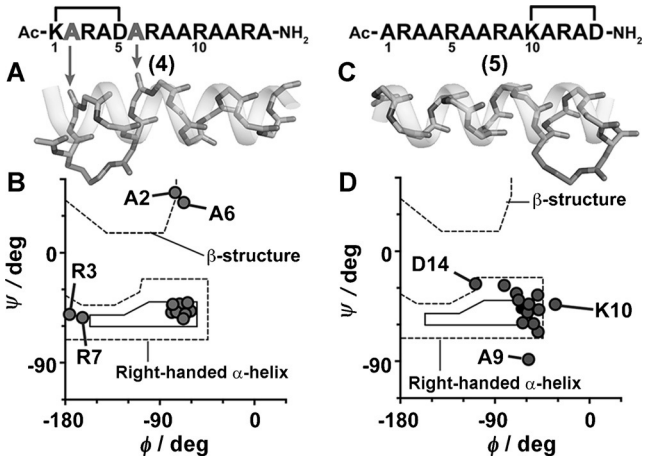

Figure 4. NMR calculated structures and Ramachandran plots for **4** and **5** (N-terminus on the left). A) Average NMR structure of **4** superimposed on an ideal α-helix (ribbon, RMSD: 1.62 Å). Arrows indicate two misaligned carbonyl oxygen atoms (Ala2, Ala6) that disrupt the hydrogen-bonding network and helix induction. B) Ramachandran plot for **4** showing two pairs of $(i,i+4)$ hydrogen-bonding partners (Ala2,Ala6; Arg3,Arg7) outside α-helix ϕ/ψ space. C) Average NMR structure of **5** superimposed on an ideal α-helix (ribbon, RMSD: 1.35 Å). All carbonyl groups are aligned for helix induction. D) Ramachandran plot showing residues in α-helical space.

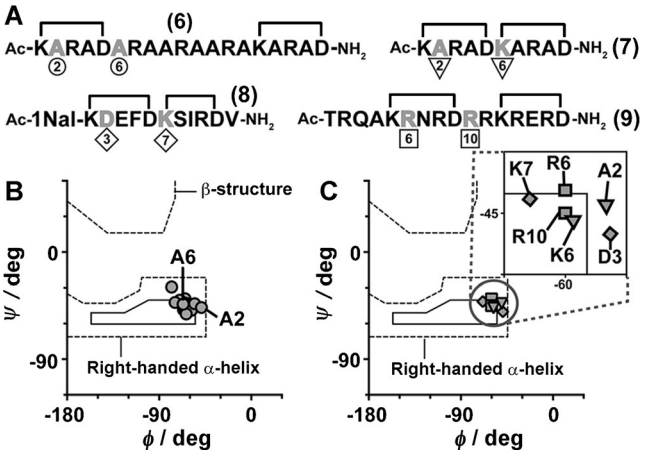

Figure 5. Correcting the helix defect in α-helical peptides. A) Sequences of α-helical peptides **6**–**9**. Residues in gray are compared in (B) and (C). B) Ramachandran plot for **6** showing all residues in α-helical space. A2 and A6 are $(i,i+4)$ hydrogen-bonding partners; thus, the helix defect in **4** (Figure 4B) is corrected in **6** (circles). C) Ramachandran plot for **7** (triangles), **8** (diamonds), and **9** (squares) showing analogous residues in α-helix ϕ/ψ space, demonstrating the correction of the helical defect in water.

value of 1.35 Å versus an idealized helix (Figure 4C; see also Figure S32B). In contrast to **4**, almost all residues of **5** occupied Ramachandran α-helical space, and although Ala9 and Lys10 were slightly distorted (Figure 4D), residues within the cycle were correctly positioned to make $(i,i+4)$ hydrogen bonds to residues further along the appended peptide chain.

The cyclic pentapeptide **2** was next attached to both ends of the palindromic peptide **3** to create Ac-(cyclo-1,5;15,19)-[KARAD]ARAARAARA[KARAD]-NH_2 **6** (Figure 5). CD spectra showed greater helicity for **6** than **4** or **5** (Figure 2). NMR data and the calculated structure for **6** (see Figure S32C and Tables S30 and S31) agreed well with CD spectra. The Ramachandran plot for **6** (Figure 5B) showed all residues in α-helical space. Thus, the attachment of macrocycle **2** to both ends of **3** overcame the minor helix distortion observed when a single unit of **2** was attached. Comparison of Ramachandran plots of Ala2 and Ala6 in **4** and **6** showed that they were now in α-helical conformations and not distorted from helicity (Figure 5B).

Next, two cyclic units placed back-to-back (**7**, **8**) or spaced by 2 or 9 residues (**9**, **6**) were examined for the potential to correct distortions observed around Asp5 in peptides **1** and **4**. We have reported bicyclic peptides Ac-(cyclo-1,5;6,10)-[KARAD][KARAD]-NH_2 (**7**),[6a] Ac-(cyclo-2,6;7,11)-1Nal-[KDEFD][KSIRD]V-NH_2 (1Nal = 1-naphthylalanine) (**8**),[6c] and Ac-(cyclo-5,9;12,16)-TRQA[KRNRD]RR[KRERD]-NH_2 (**9**),[6c] which appeared to be α-helical, but now decided to look more closely at their structures for subtle defects, as all three structures **7**–**9** had residues at positions corresponding to defects in **1** and **4** (Figure 5A, gray residues). The distorted Ramachandran coordinates for Ala2 and Ala6 in **4** (Figure 4B) all shifted into typical α-helical space for the corresponding residues in **6**–**9** (Figure 5B,C). Consistent with realignment of the carbonyl oxygen atoms, the amide $^3J_{NH-CH\alpha}$ coupling constant for Asp5 decreased from 6.9 Hz in **1** to 5.4 Hz in **4** and 4.0–4.8 Hz in **6**–**9** (see Figure S35). Their NMR structures and $^3J_{NH-CH\alpha}$ values below 6 Hz suggested that **6**–**9** all lacked the defects and were correctly aligned for continuous α-helicity (see Figure S33 and Table S34). Thus, the small structural defect at Asp5 in the highly α-helical monocycle **1**, which is magnified in longer peptide sequences and manifested by greater helix nucleation when the cycle is at the C-terminus (e.g. **5**) than when it is at the N-terminus (e.g. **4**), can be corrected by the use of a second cycle placed either alongside the first (e.g. **7**, **8**) or two (e.g. **9**) or even nine (e.g. **6**) residues away from it.

To determine the limit of C-terminal α-helix induction from the C-terminus, peptides varying in length from 5 to 21 amino acids were also appended to the N-terminus of **2** to give Ac-(cyclo-6,10)-RAARA[KARAD]-NH_2 (**10**), Ac-(cyclo-14,18)-AARAARAARAARA[KARAD]-NH_2 (**11**), Ac-(cyclo-18,22)-RAARAARAARAARAARA[KARAD]-NH_2 (**12**), and Ac-(cyclo-22,26)-ARAARAARAARAARA-ARAARA[KARAD]-NH_2 (**13**). Analogues containing the acyclic C-terminal cap -KARAD-NH_2 (**14**) instead of **2** were also synthesized for comparison (peptides **3** and **15**–**17**). CD spectra showed a small but gradual increase in helicity across both the cyclic ($f_H = 0.88$–0.98) and acyclic peptide series ($f_H = 0.05$–0.31; Figure 6A). Surprisingly, the strong α-helix induction by **2** even improved slightly with increasing peptide length, approaching near perfect α-helicity. CD spectra were also used to monitor α-helicity in cyclic **11** versus acyclic **15** in the presence of guanidine·HCl (Gdn·HCl) at increasing concentrations (Figure 6B). Nearly twice as much Gdn·HCl was required to denature 50% of **11** (3.7 M) as compared to **15** (1.9 M), and the free energy of stabilization (ΔG_{obs}) in water was calculated to be 2.3 kcal mol^{-1} for **11** versus 1.5 kcal mol^{-1} for **15**, thus supporting a more thermodynamically stable α-

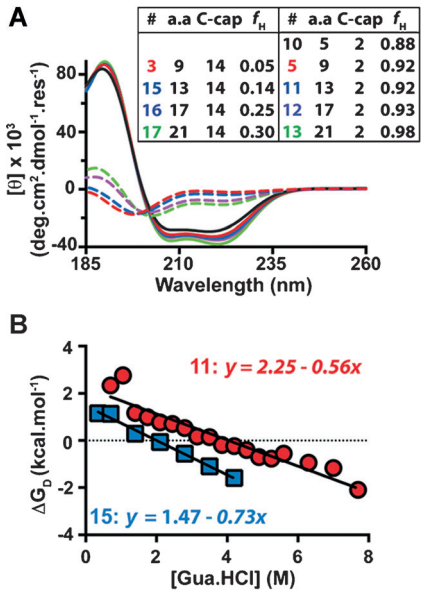

Figure 6. Helix induction from the C-terminus. A) CD spectra showing helix induction by cyclic **2** (solid lines) or acyclic **14** (dotted lines) appended to the C-terminus of peptides varying in length from 5 residues (**10**, black) to 9 (**5**, **3**, red), 13 (**11**, **15**, blue), 17 (**12**, **16**, purple), and 21 residues (**13**, **17**, green; phosphate buffer, pH 7.4, 298 K). B) Plotted change in observed free energy for **11** (circles) and **15** (squares) with increasing [Gua·HCl] (pH 7.4, 298 K).

helix in **11** as a result of the helical cycle positioned at the C-terminus. This small increase of just 0.8 kcal mol^{-1} is comparable to the reported helix stabilization energy.[5c] The amino acid tolerance for peptides capped with **2** was investigated in Ac-(cyclo-10,14)-ARAARAA**X**A[KARAD]-NH_2, X = Ala (**5**), X = Ser (**19**), X = Gly (**20**), X = Pro (**21**). CD spectra showed that helicity was dependent on the individual amino acid helix propensities (see Figure S40).

This detailed NMR and CD structure investigation has revealed a slight distortion from α-helicity at Asp5 in **1** as a result of a tight torsional restraint imposed by cyclization, which weakens one of the α-helix-defining hydrogen bonds (Figure 1). Despite this defect, **1** is far more α-helical than similar cyclic pentapeptides.[6b,d] The structural analogue **2** nucleated α-helicity very effectively from the N- or C-terminus (in peptides **4** and **5**, respectively) of peptide **3**, as assessed by CD (Figure 2) and ^{1}H NMR spectroscopy (Figures 3 and 4). Greater α-helicity was induced from the C-terminus (in peptide **5**), in contrast to most known helix nucleators, which tend to be effective only from the N-terminus.[15] Inferior N-terminal helix nucleation was due to a small distortion at the Asp5 NH group that weakened an $(i,i+4)$ hydrogen bond with Lys1 CO, thus creating a slight kink at position 6 and weakening the developing hydrogen-bonding network important for α-helicity (Figure 3, Figure 4). This kink was not present in longer peptides appended to the N-terminus of **2**; instead, all residues within the macrocycle were correctly oriented for hydrogen bonding and helix nucleation. The helix defect was repaired when two cycles were linked back-to-back in **7**,[6a] or overcome when a cycle was at both ends of a peptide (peptide **6**) or when two cycles were present (peptides **8**, **9**; Figure 5).[6c]

In conclusion, the nucleating capacity of a helical cyclic pentapeptide was found to be high when appended to either or both ends of a peptide; nucleation was more effective from the C-terminus, but equally effective when two or more helical cycles were present. These findings are important for understanding how to use constrained peptides to optimally mimic or inhibit protein–protein interactions. The nature and location of a helix-inducing constraint can profoundly alter peptide structure and protein binding. The association of subtle structural effects with an impact on helix nucleation can teach us about the consequences of small structural perturbations in proteins and guide the design of synthetic helical cycles to more effectively harness the biological activity of short peptides corresponding to bioactive protein α-helices.

Acknowledgements

We acknowledge the ARC for a Federation Fellowship (FF0668733), grants (DP1096290, DP150104609), and support through the ARC Centre of Excellence in Advanced Molecular Imaging (CE140100011), and the NHMRC for a Senior Principal Research Fellowship (APP1027369) and a grant (APP511194).

Keywords: circular dichroism · cyclic peptides · helical structures · helix nucleation · NMR spectroscopy

How to cite: *Angew. Chem. Int. Ed.* **2016**, *55*, 8275–8279
Angew. Chem. **2016**, *128*, 8415–8419

[1] a) D. J. Barlow, J. M. Thornton, *J. Mol. Biol.* **1988**, *201*, 619; b) D. P. Fairlie, M. L. West, A. K. Wong, *Curr. Med. Chem.* **1998**, *5*, 29; c) D. A. Guarracino, B. N. Bullock, P. S. Arora, *Biopolymers* **2011**, *95*, 1; d) V. Guerlavais, T. K. Sawyer, *Annu. Rep. Med. Chem.* **2014**, *49*, 331.

[2] a) K. Miyauchi, M. M. Kozlov, G. B. Melikyan, *PLoS Pathog.* **2009**, *5*, e1000585; b) X. Hu, P. Saha, X. Chen, D. Kim, M. Devarasetty, R. Varadarajan, M. M. Jin, *J. Am. Chem. Soc.* **2012**, *134*, 14642.

[3] a) R. S. Harrison, PhD dissertation, University of Queensland, **2010**; b) B. N. Bullock, A. L. Jochim, P. S. Arora, *J. Am. Chem. Soc.* **2011**, *133*, 14220.

[4] a) F. Z. Zhang, O. Sadovski, S. J. Xin, G. A. Woolley, *J. Am. Chem. Soc.* **2007**, *129*, 14154; b) H. Jo, N. Meinhardt, Y. Wu, S. Kulkarni, X. Hu, K. E. Low, P. L. Davies, W. F. DeGrado, D. C. Greenbaum, *J. Am. Chem. Soc.* **2012**, *134*, 17704; c) Y. X. Wang, D. H. C. Chou, *Angew. Chem. Int. Ed.* **2015**, *54*, 10931; *Angew. Chem.* **2015**, *127*, 11081; d) C. M. Haney, M. T. Loch, W. S. Horne, *Chem. Commun.* **2011**, *47*, 10915.

[5] a) J. W. Taylor, Q. K. Jin, M. Sbacchi, L. Wang, P. Belfiore, M. Garnier, A. Kazantzis, A. Kapurniotu, P. F. Zaratin, M. A. Scheideler, *J. Med. Chem.* **2002**, *45*, 1108; b) J. W. Taylor, *Biopolymers* **2002**, *66*, 49; c) C. Yu, J. W. Taylor, *Bioorg. Med. Chem.* **1999**, *7*, 161.

[6] a) N. E. Shepherd, G. Abbenante, D. P. Fairlie, *Angew. Chem. Int. Ed.* **2004**, *43*, 2687; *Angew. Chem.* **2004**, *116*, 2741; b) N. E. Shepherd, H. N. Hoang, G. Abbenante, D. P. Fairlie, *J. Am. Chem. Soc.* **2005**, *127*, 2974; c) R. S. Harrison, N. E. Shepherd, H. N. Hoang, G. Ruiz-Gómez, T. A. Hill, R. W. Driver, V. S. Desai, P. R. Young, G. Abbenante, D. P. Fairlie, *Proc. Natl. Acad. Sci. USA* **2010**, *107*, 11686; d) A. D. de Araujo, H. N. Hoang,

W. M. Kok, F. Diness, P. Gupta, T. A. Hill, R. W. Driver, D. A Price, S. Liras, D. P. Fairlie, *Angew. Chem. Int. Ed.* **2014**, *53*, 6965; *Angew. Chem.* **2014**, *126*, 7085.

[7] H. E. Blackwell, R. H. Grubbs, *Angew. Chem. Int. Ed.* **1998**, *37*, 3281; *Angew. Chem.* **1998**, *110*, 3469.

[8] a) C. E. Schafmeister, J. Po, G. L. Verdine, *J. Am. Chem. Soc.* **2000**, *122*, 5891 – 5892; b) L. D. Walensky, A. L. Kung, I. Escher, T. J. Malia, S. Barbuto, R. D. Wright, G. Wagner, G. L. Verdine, S. J. Korsmeyer, *Science* **2004**, *305*, 1466; c) F. Bernal, A. F. Tyler, S. J. Korsmeyer, L. D. Walensky, G. L. Verdine, *J. Am. Chem. Soc.* **2007**, *129*, 2456; d) P. S. Kutchukian, J. S. Yang, G. L. Verdine, E. I. Shakhnovich, *J. Am. Chem. Soc.* **2009**, *131*, 4622; e) G. J. Hilinski, Y. W. Kim, J. Hong, P. S. Kutchukian, C. M. Crenshaw, S. S. Berkovitch, A. Chang, S. Ham, G. L. Verdine, *J. Am. Chem. Soc.* **2014**, *136*, 12314; f) M. L. Stewart, E. Fire, A. E. Keating, L. D. Walensky, *Nat. Chem. Biol.* **2010**, *6*, 595.

[9] a) E. Cabezas, A. C. Satterthwait, *J. Am. Chem. Soc.* **1999**, *121*, 3862.

[10] a) R. N. Chapman, G. Dimartino, P. S. Arora, *J. Am. Chem. Soc.* **2004**, *126*, 12252; b) J. Liu, D. Wang, Q. Zheng, M. Lu, P. S. Arora, *J. Am. Chem. Soc.* **2008**, *130*, 4334; c) P. S. Arora, A. Patgiri, A. L. Jochim, *Acc. Chem. Res.* **2008**, *41*, 1289; d) S. Kushal, B. B. Lao, L. K. Henchey, R. Dubey, H. Mesallati, N. J. Traaseth, B. Z. Olenyuk, P. S. Arora, *Proc. Natl. Acad. Sci. USA* **2013**, *110*, 15602; e) S. E. Miller, A. M. Watkins, N. R. Kallenbach, P. S. Arora, *Proc. Natl. Acad. Sci. USA* **2014**, *111*, 6636.

[11] a) L. Guo, A. M. Almeida, W. Zhang, A. G. Reidenbach, S. H. Choi, I. A. Guzei, S. H. Gellman, *J. Am. Chem. Soc.* **2010**, *132*, 7868; b) M. D. Boersma, H. S. Haase, K. J. Peterson-Kaufman, E. F. Lee, O. B. Clarke, P. M. Colman, B. J. Smith, W. S. Horne, W. D. Fairlie, S. H. Gellman, *J. Am. Chem. Soc.* **2012**, *134*, 315; c) C. M. Goodman, S. Choi, S. Shandler, W. F. DeGrado, *Nat. Chem. Biol.* **2007**, *3*, 252; d) R. P. Cheng, S. H. Gellman, W. F. DeGrado, *Chem. Rev.* **2001**, *101*, 3219.

[12] a) V. Azzarito, K. Long, N. S. Murphy, A. J. Wilson, *Nat. Chem.* **2013**, *5*, 161; b) V. Azzarito, J. A. Miles, J. Fisher, T. A. Edwards, S. Warriner, A. Wilson, *Chem. Sci.* **2015**, *6*, 2434; c) J. Fremaux, L. Mauran, K. Pulka-Ziach, B. Kauffmann, B. Odaert, G. Guichard, *Angew. Chem. Int. Ed.* **2015**, *54*, 9816; *Angew. Chem.* **2015**, *127*, 9954.

[13] a) M. J. Kelso, H. N. Hoang, T. G. Appleton, D. P. Fairlie, *J. Am. Chem. Soc.* **2000**, *122*, 10488; b) M. J. Kelso, H. N. Hoang, W. Oliver, N. Sokolenko, D. R. March, T. G. Appleton, D. P. Fairlie, *Angew. Chem. Int. Ed.* **2003**, *42*, 421; *Angew. Chem.* **2003**, *115*, 437; c) R. L. Beyer, H. N. Hoang, T. G. Appleton, D. P. Fairlie, *J. Am. Chem. Soc.* **2004**, *126*, 15096.

[14] a) T. Cierpicki, J. Otlewski, *J. Biomol. NMR* **2001**, *21*, 249; b) G. Wagner, W. Braun, T. F. Havel, T. Schaumann, N. Go, K. Wüthrich, *J. Mol. Biol.* **1987**, *196*, 611.

[15] a) R. Austin, R. A. Maplestone, A. M. Sefler, K. Liu, W. N. Hruzewicz, C. Liu, H. S. Cho, D. E. Wemmer, P. A. Bartlett, *J. Am. Chem. Soc.* **1997**, *119*, 6461; b) B. Heitmann, G. E. Job, R. J. Kennedy, S. M. Walker, D. S. Kemp, *J. Am. Chem. Soc.* **2005**, *127*, 1690; c) K. Mueller, D. Obrecht, A. Knierzinger, C. Stankovic, C. Spiegler, W. Bannwarth, A. Trzeciak, G. Englert, A. M. Labhardt, P. Schoenholzer, *Pers. Med. Chem.* **1993**, 513.

Received: February 29, 2016
Published online: May 25, 2016

